Journal of Arid Environments 100-101 (2014) 93–99

Contents lists available at ScienceDirect

Journal of Arid Environments

journal homepage: www.elsevier.com/locate/jaridenv

Variations in tree-ring width indices over the past three centuries and their associations with sandy desertification cycles in East Asia

Ting Hua [a], Xunming Wang [b,*], Lili Lang [b], Caixia Zhang [a]

[a] Key Laboratory of Desert and Desertification, Cold & Arid Regions Environmental & Engineering Research Institute, Chinese Academy of Sciences, Lanzhou 730000, China

[b] Key Laboratory of Water Cycle & Related Land Surface Processes, Institute of Geographic Sciences and Natural Resources Research, Chinese Academy of Sciences, Beijing 100101, China

ARTICLE INFO

Article history:
Received 22 May 2013
Received in revised form
8 October 2013
Accepted 18 October 2013
Available online 7 November 2013

Keywords:
Arid and semiarid regions
Climate change
Dendrochronology
Land degradation

ABSTRACT

A database of 39 annually resolved, tree-ring width chronologies covering the Mongolian Plateau, northeastern China region, and the Yellow River drainage was established to identify variations in sandy desertification cycles over the past three centuries. Our results show that the arid, semiarid, and semi-humid East Asia experienced multiple sandy desertification cycles over the past 300 years. The Mongolian Plateau experienced sandy desertification from the 1730s to the 1750s and the 1810s to the 1910s. Northeastern China region was subject to sandy desertification from the 1700s to the 1720s, the 1770s to the 1820s, and the 1830s to the 1860s. In the Yellow River drainage, sandy desertification occurred from the 1700s to the 1730s, the 1750s to the 1780s, and the 1810s to the 1850s. The occurrence of sandy desertification was closely related to weakened summer monsoon and enhanced winter monsoon associated with decreases in precipitation and increases in aeolian activity during the Little Ice Age; reversals of sandy desertification resulted mainly from increases in precipitation and decreases in aeolian activity during the Current Warm Period. The sandy desertification cycles we reconstructed have been verified by monitoring results of modern sandy desertification trends and evidence from ancient archives and archaeological records.

1. Introduction

The Mongolian Plateau (MP), northeastern China region (NCR), and Yellow River drainage (YRD), located in arid, semiarid, and semi-humid regions of East Asia, are characterized by relative low precipitation with high inter-annual variability (Huang et al., 2011). Throughout the Holocene, frequent changes in the northern limit of the East Asia summer monsoon (Zhang et al., 2008) resulted in multiple climate changes (e.g., Cook et al., 2010; Shen et al., 2007). Such climate changes impacted human inhabitants through contributing to agricultural failures (Tao et al., 2004) and economic losses (Nkonya et al., 2011), and also led to environmental degradation through dust storms (Prospero and Lamb, 2003; Qian et al., 2002; X.Wang et al., 2004b) and desertification (Sivakumar, 2007). An important environmental issue, desertification currently jeopardizes the livelihoods of nearly 200 million people (X. Wang et al., 2008; Zhu and Chen, 1994) and had significant impacts on the subsistence of historical populations. Multiple desertification cycles that occurred in these regions (e.g., Dong et al., 1995; Wang et al., 2010) affected the livelihoods of inhabitants, impacted the prosperity and led to the abandonment of ancient cities (e.g., S.C. Wang and Dong, 2001), and may have influenced the rise and collapse of ancient Chinese dynasties (e.g., Wang et al., 2010).

The Convention to Combat Desertification and the United Nations Environment Programme (UNEP) define desertification as "land degradation in arid, semiarid and dry sub-humid areas resulting from various factors, including climatic variations and human activities" (UNEP, 1992, 1997). The term desertification mainly relates to forms such as salinization and sandy desertification (Wang, 2013). However, in China, because the areas of sandy desertification is over 80% of the total area of desertification (Shen et al., 2001), and because the key erosive force of sandy desertification is aeolian activity (Mason et al., 2008; Wang et al., 2007), the term sandy desertification and desertification are usually taken to have the same meaning. In arid, semiarid, and semi-humid regions of East Asia, the occurrence of sandy desertification mainly includes dune reactivation, coarsening of surface sediments, the desertification of grassland, and other related processes (Zhu and Chen,

* Corresponding author.
E-mail addresses: hactgexin@lzb.ac.cn (T. Hua), xunming@lzb.ac.cn, xunming_wang@yahoo.com.cn (X. Wang), langll07@lzu.edu.cn (L. Lang), zhangcaixia@lzb.ac.cn (C. Zhang).

0140-1963/$ – see front matter © 2013 Elsevier Ltd. All rights reserved.
http://dx.doi.org/10.1016/j.jaridenv.2013.10.011

1994), which are triggered mainly by variations in aeolian activities. In these regions the variations in aeolian activity can be caused by short-term severe moisture deficits (i.e., at decadal scale, Schlesinger et al., 1990), long-term aridity (e.g., Pickup, 1998), and the strengthening of wind activity (e.g., X. Wang et al., 2008). In addition, in arid, semiarid, and semi-humid regions of East Asia, results of previous studies (e.g., Wang et al., 2006) have shown that even in modern times, although human activities promoted sandy desertification, climatic changes have had a much greater effects, even though it is undeniable that human impacts have exacerbated those effects (Wang et al., 2006).

Owing to the remarkable differences in the landscape in arid, semiarid, and semi-humid East Asia, there are differences in the factors that control aeolian activity in these regions. For instance, in regions of northeastern China and the Yellow River drainage, desertification occurred mainly in regions covered by vegetated dunes, and increases in desertification was usually exhibited by anchored or semi-anchored dunes/sand sheets being reworked into mobile or semi-anchored dunes/sand sheets (Wang et al., 2008). In the Mongolian Plateau, the dominant landscape is steppe where only a few vegetated dunes are developed. Therefore, although aeolian activity in this region is still mainly controlled by wind activity, aeolian activity and the occurrence of sandy desertification are more sensitive to aridity and extremely low temperatures in winter (Sternberg et al., 2009).

In arid, semiarid, and semihumid East Asia, although the occurrence of sandy desertification is controlled mainly by climate change, its cycles in historical periods are still poorly understood. In these regions, historical climate change has already been reconstructed using natural proxies (e.g., Deng et al., 2006; Liu et al., 2002) or through documentary evidences (Ge et al., 2003; Song, 2000). Among these, tree-ring width records have been frequently employed as natural proxies (e.g., Cook et al., 2004; Mann et al., 1998) because of their high resolution, relatively low dating error, wide distribution, and explicit indications of climate change. Therefore, sampled tree-ring width indices from arid, semiarid, and semi-humid areas of East Asia are of significance for reconstructing the climate change of these regions. Based on an integrated analysis of 39 annually-resolved tree-ring width chronologies (Fig. 1; Supplementary material Table S1) and the association of their variations with indications of desertification, we report on the desertification cycles over the past three centuries in arid, semiarid, and semi-humid East Asia, and discuss their association with climate change.

2. Tree-ring dataset

We established a database of 39 annually resolved ring-width chronologies from the International Tree-Ring Data Bank (ITRDB) (http://www.ncdc.noaa.gov/paleo/treering.html) and from previous literature as described in the supplementary materials. All the chronologies in Mongolia were created using the ARSTAN program (Cook and Holmes, 1999) based on the raw measurements downloaded from the ITRDB, and were detrended using a negative exponential curve or linear regression. The detailed chronology creation processes and detrending methods from other regions are described in their source publications (Supplementary Material Table S1). All source data are standard chronologies except for chronologies 'cbb', 'cbpi', and 'cbc'. The source data was unevenly distributed throughout the MP, NCR, and YRD. Only those chronologies exhibiting statistically significant ($p < 0.10$) positive correlations with their adjacent aeolian activities index, calculated from instrumental meteorological records, or the relative humidity grid data from the National Centers for Environmental Prediction/National Center for Atmospheric Research (NCEP/NCAR) (Kalnay et al., 1996) were retained for our analysis.

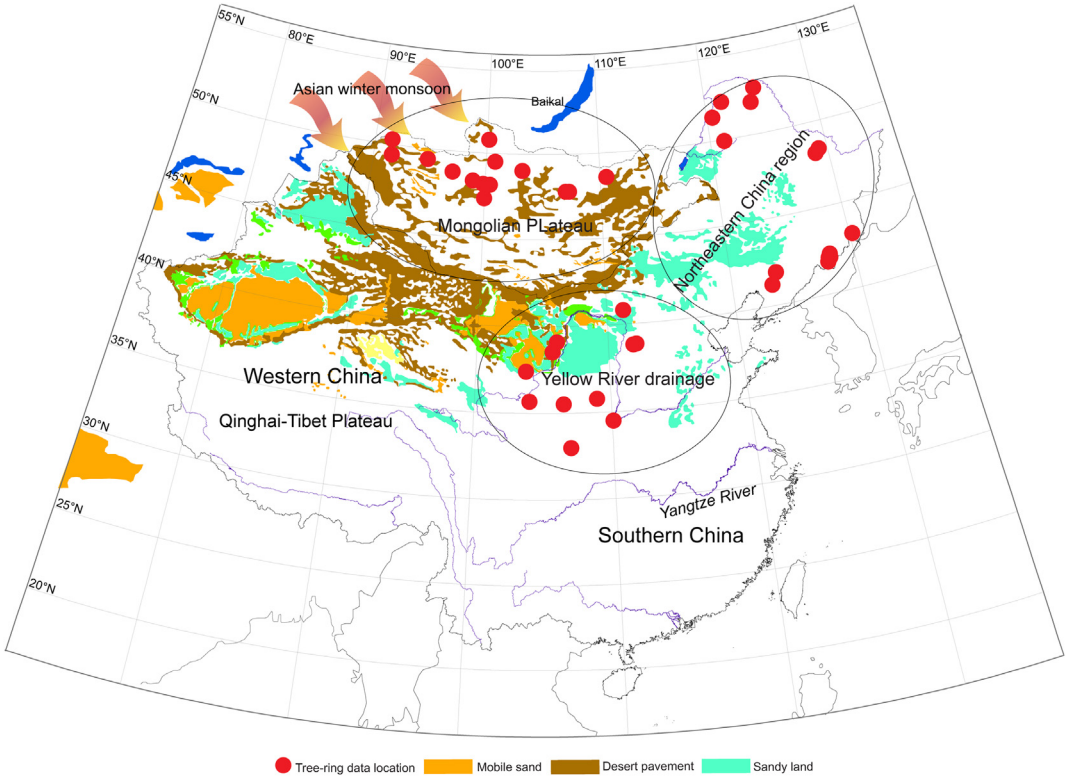

Fig. 1. Map of the Mongolian Plateau (MP), northeastern China region (NCR), and the Yellow River drainage (YRD), and sampling sites of tree-ring chronologies.

We performed Pearson's correlation tests using instrumental records at or near the sampling sites to test the sandy desertification signals included within the proxies. We used monthly mean precipitation, evaporation, and wind records with spans of approximately 50 years (1954–2000) for the meteorological data of the NCR and YRD. Because instrumental records were unavailable for the MP, we employed the NCEP/NCAR reanalysis monthly mean near-surface relative humidity grid data from January 1948 to December 2000 with a 2.5° × 2.5° spatial resolution. Since sandy desertification processes in the MP are controlled mainly by moisture conditions (e.g., Sternberg et al., 2009), it is reasonable to consider relative humidity as an indicator of sandy desertification (the details are provided in Section 3). As we were concerned about the positive correlation coefficients, we conducted one-tailed tests as suggested by Mann et al. (2008) and others. Additionally, there were significant temporal discrepancies in the responses of the tree-ring widths to climatic and environmental conditions, including aeolian processes, at the different sampling sites (Fritts et al., 1971). Therefore, we performed correlation analyses between the tree-ring chronologies and the monthly, annual, and seasonal instrumental records, as well as multiform monthly combinations. The statistical tests showed that all of the records were statistically significant at the 0.05 level, except for the 'hvr', 'tcm', 'manz', 'zm', 'th', 'cbc', 'sxnw', 'hls', and 'tbs' chronologies, which were significant at the 0.10 level (Supplementary material Table S2).

Some chronologies did not cover the entire period from 1700 to 2000, thus adjustments to bring them into phase with the longer records over the common period were necessary. Here, we employed principles described by Osborn and Briffa (2006), except that we did not scale the chronologies using standardized deviation, because the source data were of the same type of proxy with certain ranges of variance. First, the longest chronologies, which covered the full study period from 1700 to 2000, remained unchanged. The other chronologies were adjusted successively, in descending order in terms of the chronology length, using transition methods to ensure that they had the same means as the longer chronologies during periods of overlap (Equation (1)). Consequentially, all chronologies had identical means during periods that overlapped other chronologies. The adjustment methods are expressed as:

$$x_{ad_{i,j}} = x_{i,j} + \Delta\bar{x}_j, \quad where \quad \Delta\bar{x}_j = \bar{x}_{\mathrm{long}_j} - \bar{x}_j = \frac{\sum_{i=1}^{n_{\mathrm{long}_j}} x_{\mathrm{long}_{i,j}}}{n_{\mathrm{long}_j}} - \frac{\sum_{i=1}^{n_j} x_{i,j}}{n_j} \tag{1}$$

where $x_{i,j}$ denotes the source data; $x_{ad_{i,j}}$ denotes the adjusted data; i is the time counter (years); and j indicates the different chronologies. The subscript 'long' refers to chronologies with records longer than that of chronology j; n_j is the time span for chronology j; n_{long_j} is the product of the overlapped time span of the longer records for chronology j multiplied by the numbers of all longer records for chronology j; $\bar{x}_{long_j}$ is the mean for all longer records for chronology j in the period that overlapped chronology j; $x_{\mathrm{long}_{i,j}}$ refers to the values for the longer chronologies for chronology j; $\bar{x}_j$ is the arithmetic mean for chronology j; and $\Delta\bar{x}_j$ is the difference between $\bar{x}_{\mathrm{long}_j}$ and $\bar{x}_j$.

Because the original chronologies are scattered in different independent sources, all were assigned equal weights, as described by Juckes et al. (2006) and Osborn and Briffa (2006). The chronologies in the MP, NCR, and YRD were integrated into three sequences and the low-frequency component was preserved using a fast Fourier transform filter (e.g., Henriksson et al., 2012). We also performed tests to check whether the variations in the three integrated sequences were robust among the different selections of adjusted chronologies by excluding each in turn, as suggested by Juckes et al. (2006), and Osborn and Briffa (2006). The outcomes showed only slight differences among the sequences and showed no substantial changes throughout the study period (Fig. S1–S3), indicating that our statistical results had high reliability. In addition, we used the bootstrap technique (Efron, 1979) to estimate the confidence intervals for the three sequences, as suggested by Cook et al. (2004), Esper et al. (2002), and others. Due to limitations in sample sizes, it was difficult to determine a true sampling distribution from the available chronologies; the finite values available in each year were randomly resampled 1000 times with replacement with equal probabilities for using the true data, yielding 1000 bootstrap samples, from which the confidence intervals for the three sequences were estimated (Fig. 2).

3. Relationships between tree-ring width indices and modern sandy desertification cycles

Generally, in arid, semiarid, semi-humid East Asia regions, especially in the NCR and YRD, the sandy desertification is controlled by aeolian processes (e.g., Zhu and Chen, 1994), which are mainly revealed by variations in dune activity (e.g., X. Wang et al., 2008, 2009). To identify the historical sandy desertification cycles based on variations in tree-ring width indices, we examined initially the results of monitoring sandy desertification and trends of dune activity over the past 50 years (1950–2000) to determine relationships between the integrated tree-ring records and sandy desertification cycles. The Lancaster (1988) dune mobility index, which is one of the most reliable indices for measuring dune activity and sandy desertification cycles (e.g., Lancaster, 1988; Lancaster and Helm, 2000; X. Wang et al., 2009) was employed, and it is calculated as follows:

$$M = (W/(P/\mathrm{PE})) \tag{2}$$

where M is the dune mobility index; W is substituted by U^3as suggested by previous studies (Thomas et al., 2005) (where U is the mean monthly wind speed), P is the arithmetic average of P_{-1} and P_0 (where P_{-1} is the precipitation of the former month, and P_0 is the precipitation of current month), and PE is the potential evapotranspiration. Increases in the mobility index indicate increased desertification, while decreases indicate a reversal of desertification (e.g., X. Wang et al., 2009). This approach has been successfully employed in the western United States (e.g., Woodruff and Armburst, 1968) and in South Africa (e.g., Thomas et al., 2005), particularly when high-resolution data is not available or might require prohibitive amounts of computation.

Because sandy desertification occurred mainly in spring (e.g., X. Wang et al., 2008) and the precipitation, evaporation, and wind in this season are closely related to tree-ring growth as suggested by Yuan et al. (2002), Liang et al. (2001), Yin et al. (2008), and Li et al. (2003) among others, the mobility index in our study is the areal average of all the instrumental records covering either the NCR or the YRD in spring (March to May). We filtered both the mobility index (M) and ring-width index (RWI) sequences to remove variations on timescales of less than 10 years in order to maintain identical timescales to that of the sandy desertification monitoring results. Our results show that modern sandy desertification trends and variations in ring-width index, as well as the mobility index (Fig. 3a) are closely related. The RWI and M series exhibited significant anti-correlations in both the NCR and YRD ($p < 0.05$). For instance, the RWI record indicated that the NCR experienced sandy desertification from the 1950s to 1980s and reversal of desertification from the 1980s to 2000s, which appear consistent with the

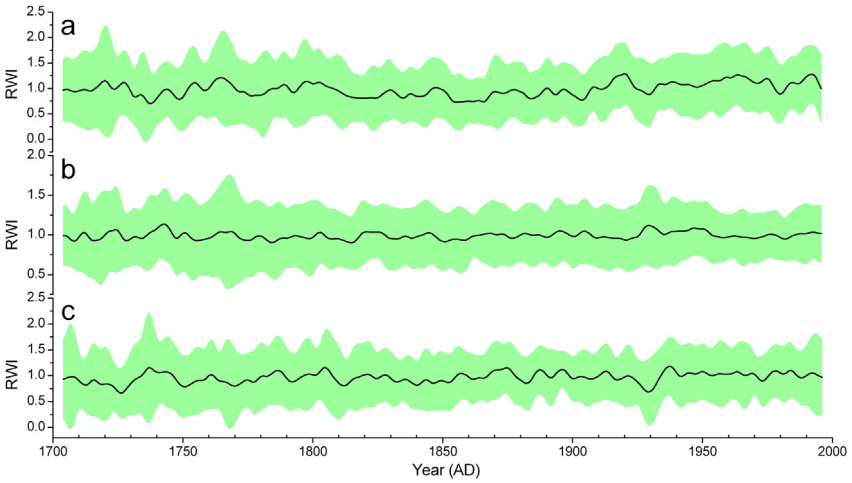

Fig. 2. The tree ring-width index sequences (black lines) and two-tailed 95% bootstrap confidence intervals (green shading) for (a) MP, (b) NCR, and (c) YRD regions from 1700 to 2000. (For interpretation of the references to colour in this figure legend, the reader is referred to the web version of this article.)

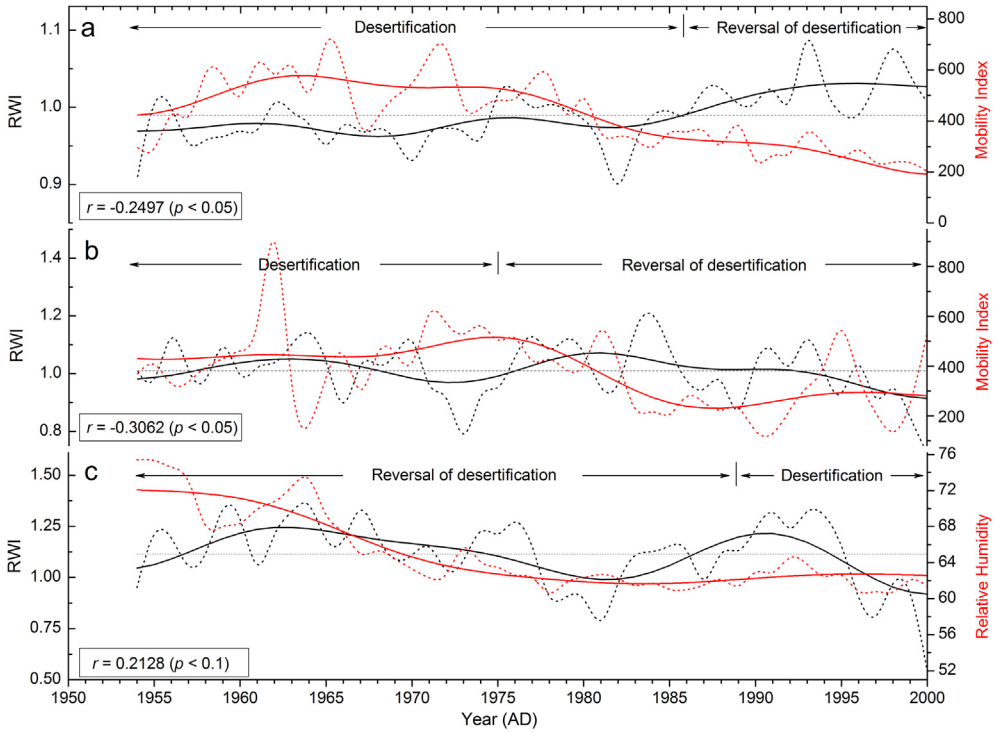

Fig. 3. Variations in the integrated RWI (black lines) and areal averages MI/relative humidity (red lines) for (a) NCR, (b) YRD, and (c) MP regions from 1950 to 2000; the decadally smoothed sequences are shown in solid lines, and their non-smoothed sequences are shown in dashed lines. The sandy desertification trends in the NCR, YRD, and MP regions were after the monitoring results of T. Wang et al. (2004), Wu (2001), and Bayarjargal et al. (2000), respectively. (For interpretation of the references to colour in this figure legend, the reader is referred to the web version of this article.)

sandy desertification trends acquired by monitoring methods (e.g., T. Wang et al., 2004). From the 1950s to the 2000s the monitoring results of the YRD (e.g., Wu, 2001) show that sandy desertification and reversal of desertification occurred in the 1970s to the 1980s and in the 1990s to the 2000s, respectively; these findings are also consistent with the RWI trends in this region (Fig. 3b). In the MP regions, because sandy desertification is more sensitive to variations in moisture conditions (Batjargal, 1996), and because of absences of data in this study, correlations between the M and the RWI are unavailable. However, our results show that variations in RWI and the relative humidity average of all grids covering the MP are closely related ($p < 0.1$) and are consistent with modern trends of sandy desertification (Fig. 3c), as suggested in previous studies (e.g., Bayarjargal, et al., 2000). Therefore, based on the integrated analyses of the RWI and its relationship to sandy desertification trends, historical cycles of sandy desertification that occurred during the past three centuries in the NCR, YRD, and MP can be reconstructed.

4. Results and discussion

Variations in the RWI of the MP, NCR, and YRD over the past three centuries are shown in Fig. 4. Although the adjusted ring-width index did not indicate the absolute amount of the radial width of the tree rings, its variations indicated relative changes in

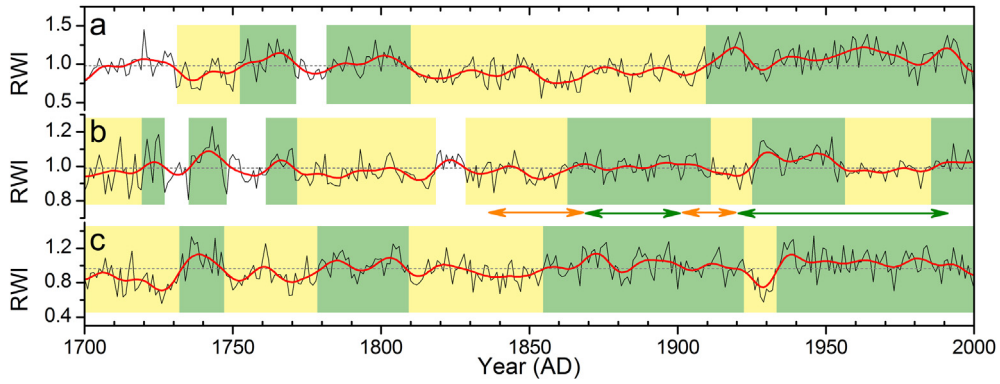

Fig. 4. Integrated tree ring-width index (RWI) records (black lines) and their decadally smoothed lines (red lines) in the MP (a), NCR (b), and the YRD (c) regions over the past three centuries. Key phases of sandy desertification and reversals of desertification derived from RWI (historical records) are indicated by yellow and green shading (arrow), respectively. The sandy desertification trends in the NCR region were after Ren and Xiao (1997). (For interpretation of the references to colour in this figure legend, the reader is referred to the web version of this article.)

aeolian processes over time. Our results showed that the MP experienced multiple sandy desertification cycles (Fig. 4a). Between the 1700s and 1910s, sandy desertification occurred from the 1730s to the 1750s and from the 1810s to the 1910s, while reversals of desertification occurred from the 1750s to the 1770s and from the 1780s to the 1810s. From the 1910s to the 2000s, reversal of desertification generally occurred throughout the MP despite some fluctuations.

From the 1700s to the 1860s, the NCR generally was subject to sandy desertification despite short-term reversals of desertification in the 1720s, from the 1740s to 1750s, and in the 1760s (Fig. 4b). From the 1860s to the present, this region was dominated by reversal of desertification, although some increased sandy desertification occurred, particularly in the 1910s to the 1920s and the 1960s to the 1990s. Our reconstructed results have been well validated in previous studies. For instance, Ren and Xiao (1997) suggested that sandy desertification occurred from 1837 to 1869 and from 1901 to 1920 in the Horqin Desert of the NCR; and reversals of desertification mainly occurred from 1869 to 1901 and from 1971 to 1990. In general, the sandy desertification cycles indicated by RWI records are highly consistent with these results; however, due to the relatively low resolution of the sandy desertification evidence, there are some slight inconsistencies in the reconstructed sandy desertification cycles.

In the YRD, sandy desertification occurred primarily during the 1700s to the 1730s, the 1750s to the 1780s, and the 1810s to the 1850s (Fig. 4c). The sandy desertification processes were triggered mainly by water shortages; this is evident because, compared with the other periods, there were significant increases in famine events during these periods (e.g., Yuan, 1994). Reversal of desertification began after the 1860s and continued into the early 2000s, except for the severe sandy desertification cycles occurring from the 1920s to the 1930s, which were also recorded in previous studies (e.g., Liang et al., 2006). Our reconstructed results for the YRD were also verified by other proxies. For instance, the Ordos Plateau of the YRD suffered sandy desertification before 1730 and reverse of desertification from 1730 to 1985 (Yang and Zhang, 1997).

The multi-taper method spectrum analysis (Mann and Lees, 1996) of three integrated RWI records in the MP, NCR, and YRD of the period from 1700 to 2000 is shown in Fig. S4. Several significant spectra peaks are identified ($p < 0.10$) at 2.3, 4.3, and 40 years in the MP (Fig. S4a); at 2.2, 3.2, and 4.2 years in the NCR (Fig. S4b); and at 2.6, 3.5, and 22–24 years in the YRD (Fig. S4c). The Mann–Kendall test shows a significant ($p < 0.05$) increasing trend in RWI records of all three regions over the past three centuries, with significant ($p < 0.05$) discrepancies between the averages before and after the start years of the abrupt change, possibly corresponding to the climate change from the Little Ice Age (LIA) to the Current Warm Period (CWP). These results confirm that most of the sandy desertification phases occurred in the LIA and reversals of desertification occurred in CWP. One possible reason for these sandy desertification cycles is that, during the LIA, weakened summer monsoons and increased winter monsoons resulted in lower precipitation (Chan and Li, 2004) and increased aeolian processes (Ding et al., 1995), and, as a result, sandy desertification occurred throughout most of arid, semiarid, and semi-humid Asia (Ci and Yang, 2004). However, during the CWP, enhanced summer monsoons and weakened winter monsoons increased precipitation (Fu and Wen, 1999) and decreased aeolian processes (e.g., Meehl et al., 1996), thus leading to reversals in desertification.

Our reconstructed results show that, over the past three centuries, there are differences in the temporal trends in the MP, NCR, and YRD. For instance, the Mann–Kennall test shows that the beginning of the abrupt change toward reversal of desertification occurred in 1939 in the MP, 1886 in the NCR, and 1797 in the YRD. Additionally, the MP experienced severe sandy desertification from the 1800s to the 1900s, while the NCR and YRD experienced reversals of desertification during most of this period (Fig. 4). Some studies (e.g., Mason et al., 2008; X. Wang et al., 2004a) suggest that responses between the landscape evolution and climate change lag in arid, semiarid, and semi-humid areas, and these lagged effects vary from area to area. Overall, however, the mechanism to account for the variations in temporal trends is poorly understood.

Previous studies (e.g., Cook et al., 2004, 2010) emphasize the close relationships between tree-ring width indices and moisture conditions. Because the dataset of this study consists of samples taken in or around the arid, semiarid, semi-humid regions of East Asia, the ring-width indices are indicative not only of the dry–wet relationship, but also illustrate significant responses to regional aeolian processes, and help identify sandy desertification cycles. Drawing on historical documents and archaeological records, S. Wang (2000), and Hou et al. (2001) among others, were able to identify sandy desertification and its reversal during certain historical periods. Our reconstructed results provide an alternate approach, which can be further refined in future studies, to identifying distinct sandy desertification cycles over the past three centuries in arid, semiarid, and semi-humid regions of East Asia.

5. Conclusions

Based on a database of 39 tree-ring width chronologies and their association with aeolian processes and historical sandy

desertification evidence, we reconstructed sandy desertification cycles over the past three centuries in regions representative of arid, semiarid, and semi-humid East Asia. Our results show that the MP experienced sandy desertification from the 1730s to the 1750s and the 1810s to the 1910s; the NCR experienced sandy desertification from the 1700s to the 1720s, the 1770s to the 1820s, and the 1830s to the 1860s; and the YRD experienced sandy desertification generally in the 1700s to the 1730s, the 1750s to the 1780s, and the 1810s to the 1850s. Sandy desertification in these three areas over the past 300 years appears closely related to weakened summer monsoon and enhanced winter monsoons; the reversal of desertification, to some degree, resulted from enhanced summer monsoon and weakened winter monsoon. In addition, our reconstructed results also show differences in the temporal trends of sandy desertification in the MP, NCR, and YRD, the mechanisms behind these differences needs to be addressed in future studies.

Acknowledgments

This work was supported by the project of the National Science and Technology Ministry (2012BAC19B09) and the National Natural Science Foundation of China (NSFC 41225001 and 41071008). We appreciated the contributors of tree-ring chronologies and their efforts on constructing the tree-ring database used in this study, which was listed in the supplementary materials. Special thanks are given to our colleagues for their critical comments on this manuscript.

Appendix A. Supplementary data

Supplementary data related to this article can be found at http://dx.doi.org/10.1016/j.jaridenv.2013.10.011.

References

Bayarjargal, Y., Adyasuren, T., Munkhtuya, S., 2000. Drought and vegetation monitoring in the arid and semi-arid regions of the Mongolia using remote sensing and ground data. Proc. 21st Asian Conf. Remote Sens. 1, 372–377.
Batjargal, Z., 1996. Nature and E Nvironment in Mongolia. Ministry of Nature and the Environment, Ulaanbaatar.
Chan, J.C.L., Li, C., 2004. The East Asia winter monsoon. In: Chang, C.P. (Ed.), East Asian Monsoon. World Scientific, Singapore, pp. 107–150.
Ci, L.J., Yang, X.H., 2004. Progress in feedback mechanism between desertification and climate change. Acta Ecol. Sin. 24 (4), 755–760 (in Chinese with English Abstract).
Cook, E.R., Anchukaitis, K.J., Buckley, B.M., D'Arrigo, R.D., Jacoby, G.C., Wright, W.E., 2010. Asian monsoon failure and megadrought during the last millennium. Science 328, 486–489.
Cook, E.R., Holmes, R.L., 1999. Program ARSTAN–chronology Development with Statistical Analysis (Users Manual for Program ARSTAN). Laboratory of Tree-Ring Research, University of Arizona, Tucson, Az.
Cook, E.R., Woodhouse, C.A., Eakin, C.M., Meko, D.M., Stahel, D.W., 2004. Long-term aridity changes in the western United States. Science 306, 1015–1018.
Deng, C.L., Shaw, J., Liu, Q.S., Pan, Y.X., Zhu, R.X., 2006. Mineral magnetic variation of the Jingbian loess/paleosol sequence in the northern Loess Plateau of China: implications for Quaternary development of Asian aridification and cooling. Earth Planet. Sci. Lett. 241, 248–259.
Ding, Z.L., Liu, T.S., Rutter, N.W., Yu, Z.W., Guo, Z.T., Zhu, R.X., 1995. Ice-volume forcing of East Asian winter monsoon variations in the past 800,000 years. Quat. Res. 44 (2), 149–159.
Dong, G., Chen, H., Wang, G., Li, X., Shao, Y., Jin, J., 1995. Evolution of deserts and sandy lands of Northern China and its relationships with climate change over the past 150 ka. Sci. China Ser. D Earth Sci. 25, 1303–1312 (in Chinese).
Efron, B., 1979. Bootstrap methods: another look at the jackknife. Ann. Stat. 7 (1), 1–26.
Esper, J., Cook, E.R., Schweingruber, F.H., 2002. Low-frequency signals in long tree-ring chronologies for reconstructing past temperature variability. Science 295 (5563), 2250–2253.
Fritts, H.C., Blasing, T.J., Hayden, B.P., Kutzbach, J.E., 1971. Multivariate techniques for specifying tree-growth and climate relationships and for reconstructing anomalies in paleoclimate. J. Appl. Meteorol. 10 (5), 845–864.
Fu, C.B., Wen, G., 1999. Variation of ecosystems over East Asia in association with seasonal, interannual and decadal monsoon climate variability. Clim. Chang. 43 (2), 477–494.
Ge, Q.S., Zheng, J.Y., Fang, X.Q., Zhang, X.Q., Zhang, P.Y., Man, Z.M., Wang, W.C., 2003. Winter half-year temperature reconstruction for the middle and lower reaches of the Yellow River and Yangtze River, China, during the past 2000 years. Holocene 13 (6), 993–940.
Henriksson, S.V., Räisänen, P., Silén, J., Laaksonen, A., 2012. Quasiperiodic climate variability with a period of 50–80 years: Fourier analysis of measurements and earth system model simulations. Clim. Dyn. 39 (7–8), 1999–2011. http://dx.doi.org/10.1007/s00382-012-1341-0.
Hou, Y., Zhou, J., Wang, Y., 2001. The natural and humane landscape in the Ordos Plateau during the Bei Wei Dynasty (386–543). J. Desert Res. 21 (2), 188–194 (in Chinese).
Huang, G., Liu, Y., Huang, R.H., 2011. The interannual variability of summer rainfall in the arid and semiarid regions of northern China and its association with the northern hemisphere circumglobal teleconnection. Adv. Atmos. Sci. 28 (2), 257–268. http://dx.doi.org/10.1007/s00376-010-9225-x.
Juckes, M.N., Allen, M.R., Briffa, K.R., Esper, J., Hegerl, G.C., Moberg, A., Osborn, T.J., Weber, S.L., Zorita, E., 2006. Millennial temperature reconstruction intercomparison and evaluation. Clim. Past Discuss. 2, 1001–1049.
Kalnay, E., Kanamitsu, M., Kistler, R., Collins, W., Deaven, D., Gandin, L., Iredell, M., Saha, S., White, G., Woollen, J., Zhu, Y., Chelliah, M., Ebsuzaki, W., Higgins, W., Janowiak, J., Mo, K.C., Ropelewski, C., Wang, J., Leetma, A., Reynolds, R., Jenne, R., Joseph, D., 1996. The NCEP/NCAR 40-year reanalysis project. Bull. Am. Meteorol. Soc. 77 (3), 437–470.
Lancaster, N., 1988. Development of linear dunes in the southwestern Kalahari, southern Africa. J. Arid Environ. 14, 233–244.
Lancaster, N., Helm, P., 2000. A test of climatic index of dune mobility using measurements from the southwestern United States. Earth Surf. Process. Landf. 25 (2), 197–207.
Li, F., Zhang, H., Zhao, L., Shirato, Y., Wang, X., 2003. Pedoecological effects of a sand-fixing poplar (Populus simonii Carr.) forest in a desertified sandy land of Inner Mongolia, China. Plant Soil 256, 431–442.
Liang, E., Liu, X., Yuan, Y., Qin, N., Fang, X., Huang, L., Zhu, H., Wang, L., Shao, X., 2006. The 1920s drought recorded by tree rings and historical documents in the semi-arid and arid areas of northern China. Clim. Chang. 79, 403–432.
Liang, E., Shao, X., Hu, E., 2001. Variation in tree ring growth indices of Picea Meyeri from the sandy land in the steppe of Inner Mongolia. Acta Phytoecol. Sin. 25 (2), 190–194.
Liu, H.Y., Xu, L.H., Cui, H.T., 2002. Holocene history of desertification along the woodland-steppe border in northern China. Quat. Res. 57 (2), 259–270.
Mann, M.E., Bradley, R.S., Hughes, M.K., 1998. Global-scale temperature patterns and climate forcing over the past six centuries. Nature 392, 779–787.
Mann, M.E., Lees, J.M., 1996. Robust estimation of background noise and signal detection in climatic time series. Clim. Chang. 33, 409–445.
Mann, M.E., Zhang, Z.H., Hughes, M.K., Bradley, R.S., Miller, S.K., Rutherford, S., Ni, F.B., 2008. Proxy-based reconstructions of hemispheric and global surface temperature variations over the past two millennia. Proc. Natl. Acad. Sci. U. S. A. 105 (36), 13252–13257.
Mason, J.A., Swinehart, J.B., Lu, H.Y., Miao, X.D., Cha, P., Zhou, Y.L., 2008. Limited change in dune mobility in response to a large decrease in wind power in semi-arid northern China since the 1970s. Geomorphology 102, 351–363.
Meehl, G.A., Washington, W.M., Erickson III, D.J., Briegleb, B.P., Jaumann, P.J., 1996. Climate change from increased CO_2 and direct and indirect effects of sulfate aerosols. Geophys. Res. Lett. 23 (25), 3755–3758.
Nkonya, E., Gerber, N., Baumgartner, P., von Braun, J., De Pinto, A., Graw, V., Kato, E., Kloos, J., Walter, T., 2011. The Economics of Desertification, Land Degradation, and Drought. IFPRI Discussion Paper 01086. Zentrum für Entwicklungsforschung, Bonn, Germany.
Osborn, T.J., Briffa, K.R., 2006. The spatial extent of 20th-century warmth in the context of the past 1200 years. Science 311 (5762), 841–844.
Pickup, G., 1998. Desertification and climate change–the Australian perspective. Clim. Res. 11, 51–63.
Prospero, J.M., Lamb, P.J., 2003. African droughts and dust transport to the Caribbean: climate change implications. Science 302 (5647), 1024–1027.
Qian, W.H., Quan, L.S., Shi, S.Y., 2002. Variations of the dust storms in China and its climatic control. J. Clim. 15 (10), 1216–1229.
Ren, G., Xiao, P., 1997. Environmental change in the last 150 years in Bakeyao, Southeastern Horqin sandland, northeast China. Geogr. Res. 16, 39–46 (in Chinese).
Schlesinger, W.H., Reynolds, J.F., Cunningham, G.L., Huenneke, L.F., Jarrell, W.M., Virginia, R.A., Whitford, W.G., 1990. Biological feedbacks in global desertification. Science 247 (4946), 1043–1048.
Shen, C.M., Wang, W.C., Hao, Z.X., Gong, W., 2007. Exceptional drought events over eastern China during the last five centuries. Clim. Chang. 85, 453–471.
Shen, Y., Zhang, K., Wang, X., 2001. Desertification. China Environmental Science Press, Beijing.
Sivakumar, M.V.K., 2007. Interactions between climate and desertification. Agric. For. Meteorol. 142, 143–155.
Song, J., 2000. Changes in dryness/wetness in China during the last 529 years. Int. J. Climatol. 20 (9), 1003–1016.
Sternberg, T., Middleton, N., Thomas, D., 2009. Pressurised pastoralism in South Gobi, Mongolia: what is the role of drought? Transaction Inst. Br. Geogr. 34 (3), 364–377.
Tao, F., Yokozawa, M., Zhang, Z., Hayashi, Y., Grassl, H., Fu, C., 2004. Variability in climatology and agricultural production in China in association with the East Asian summer monsoon and El Niño southern oscillation. Clim. Res. 28 (1), 23–30.

Thomas, D.S.G., Knight, M., Wiggs, G.F.S., 2005. Remobilization of southern African desert dunes systems by twenty-first century global warming. Nature 435 (7046), 1218–1221.
UNEP (United Nations Environment Programme), 1992. World Atlas of Desertification. Edward Arnold, Seven Oaks, UK.
UNEP (United Nations Environment Programme), 1997. In: Middleton, N.J., Thomas, D.S.G. (Eds.), World Atlas of Desertification, second ed. Edward Arnold, London.
Wang, S.C., 2000. Fastly development and causes of desertification in west Liao River basin of Inner Mongolia during the later 10 century. J. Desert Res. (3), 238–242 (in Chinese with English Abstract).
Wang, S.Y., Dong, J.B., 2001. The rise and fall of Tongwan city with the environmental change of Mu Us sandy land. Geogr. Res. 20 (3), 347–353 (in Chinese with English Abstract).
Wang, T., Wu, W., Xue, X., Zhang, Z.W., Sun, Q.W., 2004. Spatial-temporal changes of sandy desertified land during last 5 decades in northern China. Acta Geograoguca Sin. 59, 203–212 (in Chinese with English Abstract).
Wang, X.M., 2013. Sandy desertification: borne on the wind. Chin. Sci. Bull. 58 (20), 2395–2403. http://dx.doi.org/10.1007/s11434-013-5771-9.
Wang, X.M., Chen, F.H., Dong, Z.B., 2006. The relative role of climatic and human factors in desertification in semiarid China. Glob. Environ. Chang. 16, 48–57.
Wang, X.M., Chen, F.H., Hasi, E., Li, J.C., 2008. Desertification in China: an assessment. Earth-Sci. Rev. 88, 188–206.
Wang, X.M., Chen, F.H., Zhang, J.W., Yang, Y., Li, J.J., Hasi, E., Zhang, C.X., Xia, D.S., 2010. Climate, desertification, and the rise and collapse of China's historical dynasties. Hum. Ecol. 38 (1), 157–172.
Wang, X.M., Hasi, E., Zhou, Z.J., Liu, X.P., 2007. Significance of variations in the wind energy environment over the past 50 years with respect to dune activity and desertification in arid and semiarid northern China. Geomorphology 86, 252–266.
Wang, X.M., Dong, Z.B., Liu, L.C., Qu, J.J., 2004a. Sand sea activity and interactions with climatic parameters in Taklimakan Sand Sea. China. J. Arid Environ. 57, 85–98.
Wang, X.M., Dong, Z.B., Zhang, J.W., Liu, L.C., 2004b. Modern dust storms in China: an overview. J. Arid Environ. 58 (4), 559–574.
Wang, X.M., Yang, Y., Dong, Z.B., Zhang, C.X., 2009. Responses of dune activity and desertification in China to global warming in the twenty-first century. Glob. Planet. Chang. 67, 167–185.
Woodruff, N.P., Armburst, D.V., 1968. A monthly climatic factor for the wind erosion equation. J. Soil Water Conserv. 23 (3), 103–104.
Wu, W., 2001. Study on process of desertification in Mu Us sandy land for last 50 years, China. J. Desert Res. 21 (2), 164–169 (in Chinese with English Abstract).
Yang, Z., Zhang, M., 1997. Climatic and environmental changes since 800 a BP in Pojianghaizi Lake area, Ordos Plateau. Acta Sci. Nat. Univ. Normal Human 20, 74–81 (in Chinese with English Abstract).
Yin, Z., Shao, X., Qin, N., Liang, E., 2008. Reconstruction of a 1436-year soil moisture and vegetation water use history based on tree-ring widths from Qilian junipers in northeastern Qaidam Basin, northwestern China. Int. J. Climatol/ 28 (1), 37–53.
Yuan, L., 1994. Famine History of Northwest China. Gansu People's Press, Lanzhou, China (in Chinese).
Yuan, Y., Shao, X., Li, J., Li, X., Tang, F., 2002. Discussion of precipitation information in Xiagansate tree-ring chronology and 326 year precipitation reconstruction. Acta Ecol. Sin. 22, 2048–2053.
Zhang, P.Z., Cheng, H., Edwards, R.L., Chen, F.H., Wang, Y.J., Yang, X.L., Liu, J., Tan, M., Wang, X.F., Liu, J.H., An, C.L., Dai, Z.B., Zhou, J., Zhang, D.Z., Jia, J.H., Jin, L.Y., Johnson, K.R., 2008. A test of climate, sun, and culture relationships from an 1810-year Chinese cave record. Science 322 (5903), 940–942.
Zhu, Z.D., Chen, G.T., 1994. Desertification in China. Science Press, Beijing.